2024 IEEE International Conference on Robotics and Automation (ICRA 2024)
May 13-17, 2024. Yokohama, Japan

Observer-based Distributed MPC for Collaborative Quadrotor-Quadruped Manipulation of a Cable-Towed Load

Shaohang Xu[1,2], Yian Wang[1], Wentao Zhang[1], Chin Pang Ho[2], and Lijun Zhu[1]

***Abstract*— This paper presents a collaborative quadrotor-quadruped robot system for the manipulation of a cable-towed payload. In particular, we aim to solve the challenge from the unknown dynamics of the cable-towed payload. To this end, we first propose novel dynamic models for both the quadrotor and the quadruped robot, taking into account the nonlinear robot dynamics and the uncertainties associated with the cable-towed load. Moreover, we design observers for the hybrid interaction between the robots and the payload. Theoretically, the convergence of these observers is analyzed using Lyapunov functions under mild technical assumptions. Finally, we seamlessly integrate the dynamics models and the observers into a distributed Model Predictive Control (MPC) framework with kinematics limitations and collision avoidance constraints. The proposed system is validated through challenging field experiments in indoor and outdoor environments, involving push disturbances, varying and unknown payloads, uneven terrains, etc.**

I. Introduction

This paper investigates a dual-robot system, composed of a micro quadrotor and a quadrupedal robot, connected through a cable-towed mechanism for load manipulation (refer to Fig. 1). The main challenge to control such a robotic system lies in the cable-towed mechanism, where the interaction force between the load and the robot is influenced by the length of the cable. Even when considering a single agent, such as a cable-suspended quadrotor [1]–[3], the existing methods require the precise estimation of the cable state or the prior knowledge about the dynamics of the payload.

However, it is difficult, if not impossible, to obtain the accurate knowledge about the cable-towed load in real-world applications, particularly in the wild. The difficulty will amplify for a heterogeneous robot swarm, because the interaction forces between the robots become more complicated.

In this paper, we systematically address this challenge based on the observer design theory and distributed model predictive control. To the best of our knowledge, this work presents the first quadrotor-quadruped robot system manipulating a cable-towed load in the literature. Moreover, the proposed control method include the following contributions:

- The cable state is an integer variable, leading to computationally intensive, large-dimension integer programming in MPC. To address this, we introduce novel dynamics models for both the quadrotor and the quadruped robot. In particular, we propose to treat the physical interaction as an external, unknown uncertainties, which are added to the nominal dynamics.
- To handle the unknown dynamics of the cable-towed payload, we design observers for both robots. Theoretically, we prove that the estimation errors of our observers can be bounded by an arbitrarily small tolerance. The proposed observers enable the robotic system to adaptively and automatically handle varying payloads, without any prerequisite knowledge about the cable state or the load dynamics.
- We integrate the dynamics models with the proposed observers into a *distributed* MPC framework, allowing each robot to effectively compute its control inputs while simultaneously taking into account collision avoidance constraints, kinematics limitations, navigation and manipulation objectives.
- We conduct extensive field experiments to validate the proposed system. Notably, our robotic system relies solely on onboard sensors and does not rely on any ground-truth methods, such as motion capture systems. Experimental results under significant disturbances, with varying payload weights, on uneven terrains, and in wild environments, demonstrate the effectiveness of our method.

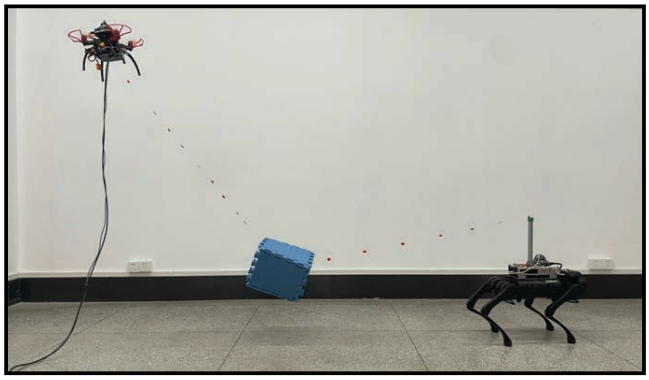

Fig. 1. The quadrotor-quadruped robot system in this paper.

The rest of this paper is structured as follows. Section II gives a brief review of related work. Section III provides a detailed introduction of the proposed control method. Section IV showcases the experimental results. Finally, Section V concludes the paper.

II. Related Work

1) Multi-Robot System: Multi-robot systems have long been a focal point in robotics research, especially in the con-

[1] School of Artificial Intelligence and Automation, Huazhong University of Science and Technology, China, shaohangxu@hust.edu.cn, yianwang@hust.edu.cn, wentaozhang@hust.edu.cn, ljzhu@hust.edu.cn
[2] School of Data Science, City University of Hong Kong, HKSAR, shaohanxu2-c@my.cityu.edu.hk, clint.ho@cityu.edu.hk

text of multiple unmanned aerial vehicles [4]–[6], multiple unmanned surface vessels [7]–[9], and multiple quadruped robots [10]–[12]. However, most methodologies are developed for *homogenous* robot systems and are not easily adaptable to our quadrotor-quadruped robot system, which is characteristically *heterogeneous* with high dimensionality, nonlinear and non-convex constraints, and significant interaction forces. In particular, most current methods tend to consider highly simplified models in controller design, however, the effective dynamics models for the quadrotor-quadruped robot system still remain to be explored.

2) Interaction between Robots: Physical interactions play a crucial role in the context of multi-robot collaboration. Generally, these interactions can be categorized as soft, hard, or hybrid. Soft interactions typically occur when dealing with soft manipulators or during the manipulation of deformable objects, which often involve complicated system dynamics [13], [14]. On the other hand, hard interactions among robots are commonly achieved through rigid linkage connections [15]–[17]. While these hard interactions are easier to model and control, the rigid connections constrain the working space, making manipulation or navigation in confined areas challenging. Our robotic system employs on a cable-towed mechanism, falling into the hybrid interactions category [18]–[20]. In contrast to hard interactions, the cable-towed mechanism allows collaborative robots to utilize greater freedom of motion, because the connection between the robots is not rigidly fixed. However, it is challenging for controller design to deal with the state of the cable, which can be either tight or loose.

3) Control for Hybrid Manipulation: A straightforward method for handling hybrid interactions is to maintain the cable in a perpetually tight state. This can be achieved by enforcing a constraint that keeps the distance between the robots equal to the length of the cable. This assumption significantly simplifies controller design, enabling collaborative manipulation through rigid formation control [20], [21]. However, similar to hard interactions, a perpetually tight cable restricts the motion capabilities of the collaborating robots.

In contrast, the hybrid mode of the cable can be effectively handled by mixed-integer programming [1], [22], [23]. In [1], a complementary constraint is proposed to describe the cable-towed dynamics, comprising a non-penetration constraint for the cable length and a limit constraint for the interaction force. This constraint is then integrated into the optimization problem, which takes into account robot dynamics, navigation objectives, and obstacle avoidance constraints. It is known that mixed-integer programming is challenging to solve in real-time. In [10], a parallelized optimization method is proposed to deal with hybrid mode switches and expedite the computation of mixed-integer programming. However, most of the current methods require the accurate knowledge of the cable-towed load, such as the position or the mass of the load. Consequently, the corresponding controllers are sensitive to inaccuracies of the dynamics models and rely on ground-truth sensors.

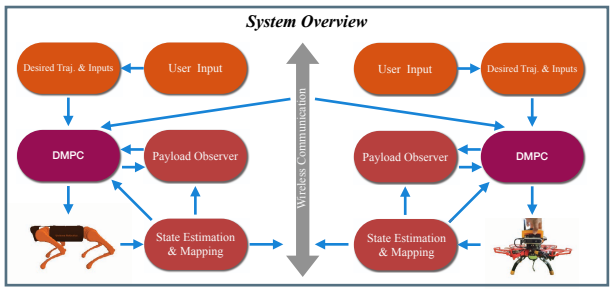

Fig. 2. The overall control system of our method. See Section III-A for the introduction.

To solve this issue, robust and adaptive control methods show promise, because they can handle cable-towed dynamics without relying on prior knowledge. For multiple cable-suspended quadrotors, an H_∞ control based method is presented in [19], which considers model parameter uncertainty and external disturbances without a precise dynamics model. However, it only considers the tight cable case and neglects physical constraints, such as collision avoidance constraints. To the best of our knowledge, observer-based MPC has never been explored for hybrid manipulation control in the literature.

III. Main Method

A. System Overview

The proposed control framework is visualized in Fig. 2. It can be seen that both robots follow a similar control pipeline. Measurements from onboard sensors are fed into the state estimation module, which computes the robot states including position, orientation, etc. A local obstacle map is subsequently generated using the registered point cloud. The payload observer utilizes the control inputs and the robot states to estimate uncertainties in robot dynamics. The two robots exchange trajectory information via wireless communication, and each robot computes its low-level control inputs through MPC. The MPC optimization problems involve the desired trajectories, the payload observers, the estimated states, and obstacle positions. Next, we will introduce the robot dynamics, observers, and MPC formulations in detail.

B. Robot Dynamics under Uncertainty

1) Nonlinear Quadruped Dynamics under Uncertainty

Our quadruped robot model builds on the centroidal dynamics model with full kinematics [24]. This model can balance the computational complexity between full-order models and highly simplified models, and has been successfully employed in dynamic locomotion on challenging terrains [25], [26]. The robot state and the control input are defined as

$$x \triangleq \mathrm{col}\{\theta, p, \omega, v, q\},$$
$$u \triangleq \mathrm{col}\{f_1, f_2, f_3, f_4, v^j\},$$

where $\theta \in \mathbb{R}^3$ is the base orientation in Euler angles, $p \in \mathbb{R}^3$ is the position of the center of mass in the world frame, $\omega \in \mathbb{R}^3$ is the base angular velocity, $v \in \mathbb{R}^3$ is the linear

velocity of the center of mass, $q \in \mathbb{R}^{12}$ is the vector of joint positions, $v^j \in \mathbb{R}^{12}$ denotes the vector of joint velocities, $f_i \triangleq \text{col}\{f_i^x, f_i^y, f_i^z\} \in \mathbb{R}^3$ is the ground reaction force of the foot i in the body frame with its projection into the x-, y- and z-axis f_i^x, f_i^y, f_i^z.

In this paper, we further introduce uncertainties into the original centroidal dynamics, which can be explained as the impact of the cable-towed payload for the nominal dynamics. The dynamical equations of the quadruped robot are:

$$\dot{\theta} = T(\theta)\omega \tag{1a}$$
$$\dot{p} = R(\theta)v \tag{1b}$$
$$\dot{\omega} = I^{-1}(-\omega \times I\omega + \sum_{i=1}^{4} r_i(q) \times f_i) + \tau_1 \tag{1c}$$
$$\dot{v} = g(\theta) + \frac{1}{m}\sum_{i=1}^{4} f_i + \tau_2 \tag{1d}$$
$$\dot{q} = v^j \tag{1e}$$

where $T(\theta) \in \mathbb{R}^{3\times3}$ is the mapping matrix from the base angular velocity $\omega \in \mathbb{R}^3$ to $\dot{\theta}$, $R(\theta) \in \mathbb{R}^{3\times3}$ is the rotation matrix from the base to the world frame, $I \in \mathbb{R}^{3\times3}$ is the inertia about the center of mass, $r_i(q) \in \mathbb{R}^3$ is the position of the foot $i \in \{1, \cdots, 4\}$ with respect to the center of mass, $g(\theta) \in \mathbb{R}^3$ is the gravitational acceleration in the body frame, $\tau_1, \tau_2 \in \mathbb{R}^3$ are both unknown uncertainties caused by the cable-towed payload.

2) On-Manifold Quadrotor Dynamics under Uncertainty

Our quadrotor model builds on the on-manifold dynamics model [27]. Compared to Euler-angle-based models and quaternion-based models, the on-manifold dynamics model is both singularity-free and minimal-parameterized, and has been applied for aggressive trajectory tracking control [27]. Similar to [27], our quadrotor employs the autopilot Pixhawk 4 (PX4) Mini, and its control input is defined as

$$u^q \triangleq \text{col}\{a^q, \omega^q\} \in \mathbb{R}^4,$$

where $a^q \in \mathbb{R}$ is the thrust acceleration and $\omega^q \in \mathbb{R}^3$ is the body angular rate. We use the superscript q to distinguish the state/control variables of the quadrotor from that of the quadruped robot. The quadrotor state is defined as

$$x^q \triangleq \text{col}\{p^q, v^q, R^q\} \in \mathbb{R}^6 \times SO(3),$$

where $R^q \in SO(3)$ is the orientation from the global to body frame, $p^q \in \mathbb{R}^3$ and $v^q \in \mathbb{R}^3$ are the body position and linear velocity in the global frame, respectively. Then, we describe the quadrotor dynamics in our dual-robot system as:

$$\dot{p}^q = v^q + \tau_1^q, \tag{2a}$$
$$\dot{v}^q = g - aR^q e_3 + \tau_2^q, \tag{2b}$$
$$\dot{R}^q = R^q \lfloor \omega^q \rfloor + \tau_3^q, \tag{2c}$$

where $g \triangleq [0, 0, 9.81]^\top$ is the gravity vector in the global frame, $e_3 \triangleq [0, 0, 1]^\top$ is the selection vector, the notation $\lfloor \cdot \rfloor$ is the skew-symmetric operator, $\tau_1^q, \tau_2^q, \tau_3^q \in \mathbb{R}^3$ represent unknown uncertainties caused by the cable-towed interaction mechanism.

Note that both (2b) and (2c) are on-manifold and cannot be computed directly in the context of nonlinear MPC. Similar to [27], we reformulate the original dynamics into the error-state dynamics by utilizing the desired states. Let us define the error terms as follows:

$$\delta v^q(t) \triangleq v^q(t) - v^{qd}(t), \tag{3a}$$
$$\delta a^q(t) \triangleq a^q(t) - a^{qd}(t), \tag{3b}$$
$$\delta \omega^q(t) \triangleq \omega^q(t) - \omega^{qd}(t), \tag{3c}$$
$$\delta R^q(t) \triangleq \text{Log}((R^{qd}(t))^{-1} R^q(t)). \tag{3d}$$

where the superscript qd represents the desired value for the related quadrotor state/control variables. Then, we employ the first-order approximation techniques for manifolds introduced in [27], [28], to reformulate the original on-manifold dynamics (2) into the following linearized and discrete-time forms:

$$p^q(t+1) = p^q(t) + (\delta v^q(t) + v^{qd}(t) + \tau_1^q(t))\Delta t, \tag{4a}$$
$$\begin{aligned}\delta v^q(t+1) = \delta v^q(t) + a^{qd}(t)R^{qd}(t)\lfloor e_3 \rfloor \delta R^q(t)\Delta t \\ - \delta a^d(t) R^{qd}(t) e_3 \Delta t,\end{aligned} \tag{4b}$$
$$\delta R^q(t+1) = \text{Exp}(-w^{qd}(t)\Delta t)\delta R^q(t) + \delta\omega(t)\Delta t, \tag{4c}$$

where Δt stands for the time interval between t and $t+1$.

The above linearization incorporates two numerical techniques: (1) projection from the manifold to the homoeomorphic space around the desired states, and (2) approximation using the first-order Taylor expansion. Note that there is only one uncertainty variable, $\tau_1^q(t)$, remaining in the reformulated equations. This is achieved by assuming $\tau_2^q(t) = \tau_2^{qd}(t)$ and $\tau_3^q(t) = \tau_3^{qd}(t)$. Detailed mathematical derivations are omitted here due to the page limit, but interested readers can refer to [27].

Remark 1. *Different from [27], we only make the error-state reformulations for v^q and R^q to address the on-manifold dynamics. As for p^q, we retain its original formulation, mainly for two reasons: (i) the original dynamical equation (2a) is linear, facilitating its integration as a linear constraint in MPC; (ii) p^q itself is crucial for navigation and collaboration. Then, we can use p^q directly in the objective function and collision-free constraints for the following MPC.*

C. Payload Observer

We aim to design the observers for the uncertainties in our dynamics models (1) and (4). To this end, we first make the following assumption about the uncertainties τ_1^q, τ_1 and τ_2.

Assumption 1. *Suppose that there exist locally Lipschitz functions ϕ_1^q, ϕ_1, ϕ_2, such that*

$$\dot{\tau}_1^q = \phi_1^q(x^q, u^q), \tag{5a}$$
$$\dot{\tau}_1 = \phi_1(x, u), \tag{5b}$$
$$\dot{\tau}_2 = \phi_2(x, u), \tag{5c}$$
$$\|\phi_1^q(x,u) - \hat{\phi}_1^q(z,u)\| \le L_1^q\|x - z\| + M_1^q, \tag{5d}$$
$$\|\phi_1(x,u) - \hat{\phi}_1(z,u)\| \le L_1\|x - z\| + M_1, \tag{5e}$$
$$\|\phi_2(x,u) - \hat{\phi}_2(z,u)\| \le L_2\|x - z\| + M_2. \tag{5f}$$

where $\hat{\phi}_1^q$, $\hat{\phi}_1$ and $\hat{\phi}_2$ are some predefined estimation functions, $L_1^q, L_1, L_2, M_1^q, M_1, M_2$ are nonnegative constants.

Remark 2. *Note that this assumption is common in the observer design theory [29]. The ground-truth sensors may provide precise or even perfect estimation, which could be used directly as $\hat{\phi}_1^q$, $\hat{\phi}_1$ and $\hat{\phi}_2$. However, in this paper, we do not assume there is any prior knowledge of the cable-towed payload, and thus we simply let all the estimation functions to be zero. To balance the ground-truth method and our method, an alternative way may be to pre-train a neural network as the empirical estimation.*

Then, we can design the observers $\hat{\tau}_1^q$, $\hat{\tau}_1$ and $\hat{\tau}_2$ for τ_1^q, τ_1 and τ_2 as:

$$\dot{\hat{\tau}}_1^q = \frac{\alpha_1}{\epsilon^2}(p^q - \hat{p}^q) + \hat{\phi}_1^q(x^q, u^q), \tag{6a}$$

$$\dot{\hat{\tau}}_1 = \frac{\beta_1}{\epsilon^2}(\omega - \hat{\omega}) + \hat{\phi}_1(x, u), \tag{6b}$$

$$\dot{\hat{\tau}}_2 = \frac{\gamma_1}{\epsilon^2}(v - \hat{v}) + \hat{\phi}_2(x, u), \tag{6c}$$

where $\epsilon \in (0, 1)$, $\alpha_1, \beta_1, \gamma_1$ are positive gains, and the auxiliary variables $\hat{p}^q, \hat{\omega}, \hat{v}$ evolve as

$$\dot{\hat{p}}^q = \frac{\alpha_2}{\epsilon}(p^q - \hat{p}^q) + \delta v^q + v^{qd} + \hat{\tau}_1^q, \tag{7a}$$

$$\dot{\hat{\omega}} = \frac{\beta_2}{\epsilon}(\omega - \hat{\omega}) + I^{-1}(-\omega \times I\omega + \sum_{i=1}^{4} r_i(q) \times f_i) + \hat{\tau}_1, \tag{7b}$$

$$\dot{\hat{v}} = \frac{\gamma_2}{\epsilon}(v - \hat{v}) + g(\theta) + \frac{1}{m}\sum_{i=1}^{4} f_i + \hat{\tau}_2, \tag{7c}$$

with the positive gains $\alpha_2, \beta_2, \gamma_2$. Next, we give a theoretical analysis on the estimation error of the proposed observers.

Proposition 1. *Under Assumption 1, there exists a small ϵ, such that the estimation errors of the observers (6) can be bounded by*

$$\|\tau_1^q - \hat{\tau}_1^q\| \le \max\{b_1^q e^{-c_1^q t/\epsilon} d_1^q, \epsilon e_1^q M_1^q\}, \tag{8a}$$

$$\|\tau_1 - \hat{\tau}_1\| \le \max\{b_1 e^{-c_1 t/\epsilon} d_1, \epsilon e_1 M_1\}, \tag{8b}$$

$$\|\tau_2 - \hat{\tau}_2\| \le \max\{b_2 e^{-c_2 t/\epsilon} d_2, \epsilon e_2 M_2\}, \tag{8c}$$

where $\forall t \ge 0$, and $b_1^q, c_1^q, d_1^q, e_1^q, b_1, c_1, d_1, e_1, b_2, c_2, d_2, e_2$ are some positive constants.

Proof. Please see the Appendix. □

Remark 3. *Note that the estimation error can be arbitrarily small by choosing a small enough ϵ. In particular, if the payload dynamics are perfectly known (e.g., through ground-truth sensors), we can prove that the estimation error exponentially converge to zero. To show this, we take τ_1 as an example. If the payload dynamics are known as a prior, we have $M_1 = 0$ in Assumption 1 since $\phi_1(x, u) = \hat{\phi}_1(x, u)$. Then, from (8b) we known that $\hat{\tau}_1$ tends to be τ_1, i.e., the estimation error tends to be zero.*

Based on the above analysis, we can conclude that the designed observers can accurately estimate the impacts of the cable-towed payload for the robots in theory.

D. Distributed MPC

Our control objective is to compute control inputs based on a high-level reference, taking into account the robot dynamics, the navigation goal, the manipulation task, and collision avoidance constraints. To this end, we leverage distributed MPC, which offers an efficient approach for integrating multiple objectives and equality/inequality constraints into mathematical programs. For both the quadruped robot and the quadrotor, we formulate different MPC optimization problems, enabling each robot to independently calculate its control inputs without relying on a centralized controller.

1) Quadruped Robot

At time step t, we formulate the following optimization problem for the quadruped robot:

$$\begin{aligned}
\min_{u(\cdot|t)} \quad & \sum_{l=0}^{N-1} (\|x(t+l|t) - x^d(t+l|t)\|_{L_x} \\
& + \|u(t+l|t) - u^d(t+l|t)\|_{L_u}) \\
& + \|x(t+N|t) - x^d(t+N|t)\|_{L_N}, && \text{(9a)} \\
\text{s.t.} \quad & x(t+1+l|t) = f(x(t+l|t), u(t+l|t), \hat{\tau}_1(t), \hat{\tau}_2(t)), && \text{(9b)} \\
& \|p(t+l|t) - p^q(t+l|t)\| \ge r_1, && \text{(9c)} \\
& \|p(t+l|t) - p_o(t+l|t)\| \ge r_2, && \text{(9d)} \\
& \mu_c f_i^z(t+l|t) \ge \sqrt{(f_i^x(t+l|t))^2 + (f_i^y(t+l|t))^2}, && \text{(9e)} \\
& f_j(t+l|t) = 0, && \text{(9f)} \\
& \forall l \in \{0, 1, \cdots, N-1\}, \forall i \in \mathcal{C}, \forall j \notin \mathcal{C}, \forall o \in \mathcal{O},
\end{aligned}$$

where the symbol $t+l|t$ denotes the corresponding variable at time $t+l$ predicted at time t, the predictive horizon is N, x^d and u^d denote the reference trajectories for the state and control inputs, respectively, L_x, L_u and L_N are weight matrices, $f(\cdot)$ represents the quadruped robot dynamics (1) with the original uncertainties τ_1 and τ_2 replaced by $\hat{\tau}_1$ and $\hat{\tau}_2$ in (6), r_1 is the safe distance between two robots, p_o is the position of the o-th obstacle, r_2 is the safe distance between the robot and the obstacle, μ_c is the friction coefficient, $\mathcal{C}$ is the set containing all the contact leg indexes, $\mathcal{O}$ is the set containing all the obstacle indexes.

The motivation of this optimization problem is illustrated as follows. The optimization objective (9a) seeks to minimize the differences between the predictive and desired states and control inputs, in order to guide the robot to its final goal position. The equality constraint (10b) represents the robot dynamics (1) using the proposed observer (6), enabling the robot to adaptively respond to the cable-towed payload. Notably, we do not have future information about τ_1 and τ_2. To address this issue, we assume τ_1 and τ_2 remain constant during the predictive horizon and use the observers at time step t, namely $\hat{\tau}_1(t)$ and $\hat{\tau}_2(t)$. The inequality constraints (9c) and (9d) are designed to prevent the quadrotor-quadruped collision or the robot-obstacle collision. The inequality constraints (9e) represent the friction cones for the contact legs, while the constraints (9f) guarantee that the contact forces

of the swing legs are zero.

The problem (9) is nonlinear and non-convex, and we leverage a sequential quadratic programming algorithm [25] to solve the above optimization program in real-time. To map the optimized ground reaction forces to joint-level torques, we utilize a whole-body controller [30] that takes into consideration the full nonlinear rigid body dynamics. The desired joint torques are subsequently achieved by the low-level motor controllers on the quadruped robot.

2) Quadrotor

The MPC problem for the quadrotor follows the same design motivation with the quadruped robot:

$$\begin{aligned}
\min_{\delta u^q(\cdot|t)} \quad & \sum_{l=0}^{N^q-1} \big(\|x^q(t+l|t) - x^{qd}(t+l|t)\|_{L_{x^q}} \\
& + \|\delta u^q(t+l|t)\|_{L_{u'}} \\
& + \|p(t+l|t) - p^q(t+l|t) - p^d\|_{L_{p^q}}\big) \\
& + \|x^q(t+N|t) - x^{qd}(t+N|t)\|_{L_{N^q}}, && \text{(10a)} \\
\text{s.t. } & x^q(t+1+l|t) = f^q(x^q(t+l|t), \delta u^q(t+l|t), \hat{\tau}_1^q(t)), && \text{(10b)} \\
& \|p(t+l|t) - p^q(t+l|t)\| \geq r_1, && \text{(10c)} \\
& \|p^q(t+l|t) - p_o(t+l|t)\| \geq r_2, && \text{(10d)} \\
& \delta u^q(t+l|t) \geq u^q_{\min} - u^{qd}(t+l|t) && \text{(10e)} \\
& \delta u^q(t+l|t) \leq u^q_{\max} - u^{qd}(t+l|t) && \text{(10f)} \\
& \forall l \in \{0, 1, \cdots, N^q - 1\}, \forall o \in \mathcal{O},
\end{aligned}$$

where $\delta u \triangleq \text{col}\{\delta a^q, \delta\omega^q\}$, p^d is the desired relative position between the quadrotor and the quadruped robot, $f^q(\cdot)$ represents the quadrotor dynamics (4) with the original uncertainties τ_1^q replaced by $\hat{\tau}_1^q$ in (6), $u^q_{\min}$ and $u^q_{\max}$ are the lower and upper bound of the control input, respectively.

In (10), we try to reduce the relative position error as part of the optimization objective. Specifically, this objective aims to maintain a *soft* formation, which is defined by p^d. In contrast to *hard* formation control, such as [20], [21], our MPC allows both the robots to exploit greater motion capabilities, which is particularly useful in coordinating navigation, manipulation, and collision avoidance. The constraints (10e) and (10f) are from the physical limits of the control inputs, while the other components in (10) are similar to those in (9).

The optimal value of δu is mapped into the original control signals a^q and ω based on the error-state definitions (3). We map the thrust acceleration command a^q to the throttle command by leveraging a calibrated hovering throttle, and the desired throttle and the body angular rate are finally achieved by the low-level controller in the PX4 mini.

IV. Experiments

A. Experiment Setup

The hardware configuration of our robotic system is depicted in Fig. 1. The Unitree A1 robot has 18 degrees of freedom with a weight of approximately 12 kilograms, while the customized micro quadrotor weighs around 1.8 kilograms. These two robots are connected to a load using monofilament fishing lines.

Our objective is to achieve collaborative manipulation both indoors and outdoors without GNSS signals. To accomplish this, each robot is equipped with a solid-state LiDAR sensor for localization and mapping. Regarding the quadrotor, we employ the Fast-LIO2 algorithm [32] directly for odometry computation. For the quadruped robot, we tightly integrate the measurements from LiDAR, IMU, and legged kinematics to estimate the robot states.

Note that the MPC problem of one robot utilizes trajectory information from the other. To facilitate data exchange through wireless communication, we have established a 5G WiFi on the quadruped robot.

B. Results and Discussion

We conducted several experiments to demonstrate the effectiveness of our control framework, and snapshots of these experiments are shown in Fig. 3.

1) Indoor and Outdoor Environments: In these experiments, the robots transported a payload along the x-axis in the global frame for 4 meters. We conducted tests in both indoor (Fig. 3 (a)) and outdoor (Fig. 3 (b)) environments. In Fig. 4(a), we illustrate the behavior of the quadrotor in terms of the robot body positions in outdoor environments. Note that the quadrotor takes off at around 8 [s] and the navigation begins at around 24 [s]. This test shows that our control method is effective without relying on any ground-truth sensors and is robust in the wild environments.

2) Collision Avoidance: In this test, we placed an obstacle wall in front of the initial robot location, and the target goal is set behind the wall (Fig. 3 (c)). Trajectories for both the quadrotor and the quadruped robot can be observed in Fig. 4(b). The results demonstrate that the robot system can successfully navigate around the obstacle while carrying the load to the destination.

3) Push Disturbance: In this experiment, we subjected the quadruped robot to lateral thrust multiple times (Fig. 3 (d)). The trajectory of the quadruped robot is depicted in Fig. 4(c). The results highlight the robustness of our control system in effectively handling unknown disturbances.

4) Terrain Uncertainty: The quadruped robot traversed unstructured blocks during the test (Fig. 3 (e)). The orientation of the quadruped robot is shown in Fig. 4(d). The results show that the quadruped robot is able to maintain its balance during the collaborative manipulation, and our control system is effective to deal with terrain uncertainties.

5) Variant Payloads: In this test, the initial payload is around 1.5 kilograms. Then, during the navigation, we added an extra load weighing approximately 2 kilograms on the top of the original payload (Fig. 3 (f)). This experiment demonstrates that our control method can automatically respond to variant payloads without requiring prior knowledge of the related dynamics.

V. Conclusion

In this paper, we introduced a distributed adaptive model predictive control framework for a novel dual-robot system

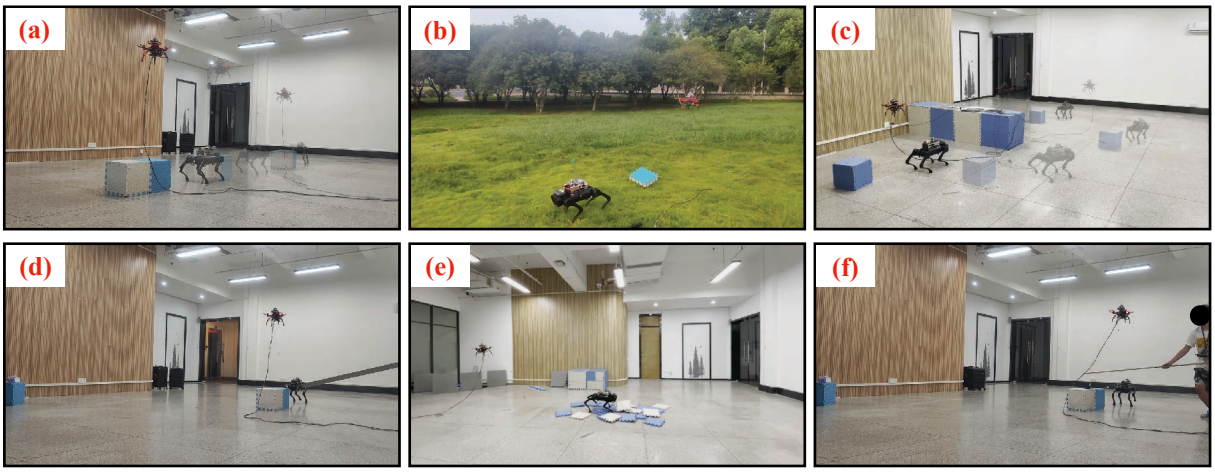

Fig. 3. The snapshots of the (a) indoor experiment, (b) outdoor experiment, (c) experiment with obstacle, (d) experiment with push disturbance, (e) experiment on unstructured blocks, and (f) experiment with variant payloads. Videos are available online [31].

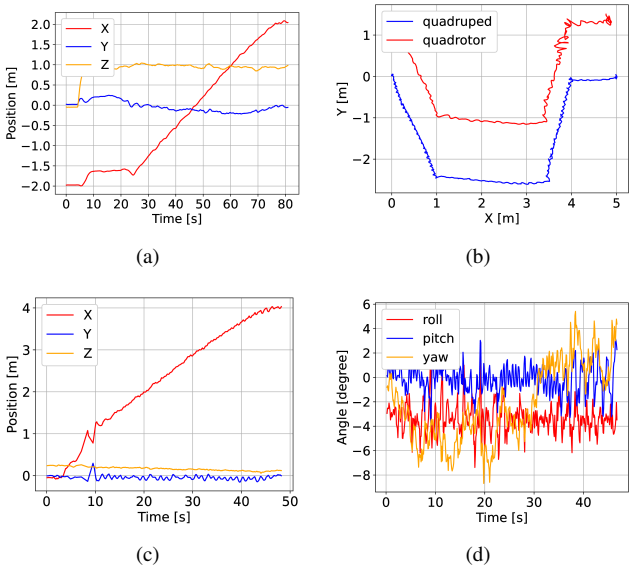

Fig. 4. (a) The trajectory of the quadrotor in the outdoor experiment. (b) The 2D trajectories of the quadrotor and the quadruped robot in the collision avoidance experiment. (c) The trajectory of the quadruped robot in the push disturbance experiment. (d) The orientation of the quadruped robot in the uneven terrain experiment.

comprising a quadrotor and a quadruped robot, enabling collaborative manipulation of a cable-towed load. In robot dynamics models, we proposed to use unknown uncertainties to describe the interaction between the robots. Then, we design observers to estimate these uncertainties online without relying on any prior knowledge. Furthermore, we presented distributed MPC optimization problems for each robot to compute control laws, incorporating constraints related to collision avoidance, navigation, and collaboration. Our extensive experiments demonstrated the robustness of this approach in the terms of terrain uncertainty, variant payloads, and external disturbances.

ACKNOWLEDGMENT

This work was supported by the National Natural Science Foundation of China under Grant 62173155, 52188102, 62225306, U2141235, Program for HUST Academic Frontier Youth Team, the CityU Start-Up Grant (Project No. 9610481), and Chow Sang Sang Group Research Fund sponsored by Chow Sang Sang Holdings International Limited (Project No. 9229076).

APPENDIX

Proof of Proposition 1:

Proof. Let us first deal with τ_1. Let us define $\tilde{\omega} \triangleq \omega - \hat{\omega}$, $\tilde{\tau}_1 = \tau_1 - \hat{\tau}_1$, and $\eta \triangleq \text{col}\{\tilde{\omega}/\epsilon, \tilde{\tau}_1\}$. Then from (6b) and (7b), we have

$$\dot{\eta} = A\eta + \epsilon B\tilde{\phi}(x,u)$$

where $\tilde{\phi}(x,u) \triangleq \phi_1(x,u) - \hat{\phi}_1(x,u)$,

$$A \triangleq \begin{bmatrix} -\beta_2 & 1 \\ -\beta_1 & 0 \end{bmatrix} \otimes I_3, B = \begin{bmatrix} 0 \\ 1 \end{bmatrix} \otimes 1_3,$$

$\otimes$ denotes Kronecker product, I_3 denotes the identity matrix with the size 3×3, and 1_3 denotes a 3-dimensional column vector with all elements being 1. The Lyapunov function is selected as $V = \eta^\top P\eta$, where P is the solution of

$$PA + A^\top P = -I_6.$$

Then, if $\epsilon L_1 \|PB\| \leq \frac{1}{4}$, we have

$$\epsilon\dot{V} \leq -\frac{1}{2}\|\eta\|^2 + 2\epsilon M_1 \|PB\|\|\eta\|.$$

Therefore, taking $d_1 \triangleq \|\text{col}\{\omega(0), \tau_1(0)\}\|$, we have some positive constants b_1, c_1 and e_1, such that

$$\|\tilde{\tau}_1\| \leq \max\{b_1 e^{-c_1 t/\epsilon} d_1, \epsilon e_1 M_1\},$$

i.e, (8b). Similarly, we can also prove (8a) and (8c). □

REFERENCES

[1] P. Foehn, D. Falanga, N. Kuppuswamy, R. Tedrake, and D. Scaramuzza, "Fast trajectory optimization for agile quadrotor maneuvers with a cable-suspended payload," in *Robotics: Science and Systems XIII*, 2017.

[2] S. Tang, V. Wüest, and V. Kumar, "Aggressive flight with suspended payloads using vision-based control," *IEEE Robotics and Automation Letters*, vol. 3, no. 2, pp. 1152–1159, 2018.

[3] J. Zeng, P. Kotaru, M. W. Mueller, and K. Sreenath, "Differential flatness based path planning with direct collocation on hybrid modes for a quadrotor with a cable-suspended payload," *IEEE Robotics and Automation Letters*, vol. 5, no. 2, pp. 3074–3081, 2020.

[4] K. Sreenath and V. Kumar, "Dynamics, control and planning for cooperative manipulation of payloads suspended by cables from multiple quadrotor robots," in *Robotics: Science and Systems IX*, 2013.

[5] M. Gassner, T. Cieslewski, and D. Scaramuzza, "Dynamic collaboration without communication: Vision-based cable-suspended load transport with two quadrotors," in *2017 IEEE International Conference on Robotics and Automation (ICRA)*. IEEE, 2017, pp. 5196–5202.

[6] G. Li, R. Ge, and G. Loianno, "Cooperative transportation of cable suspended payloads with mavs using monocular vision and inertial sensing," *IEEE Robotics and Automation Letters*, vol. 6, no. 3, pp. 5316–5323, 2021.

[7] B.-B. Hu, H.-T. Zhang, B. Liu, H. Meng, and G. Chen, "Distributed surrounding control of multiple unmanned surface vessels with varying interconnection topologies," *IEEE Transactions on control systems Technology*, vol. 30, no. 1, pp. 400–407, 2021.

[8] B.-B. Hu and H.-T. Zhang, "Bearing-only motional target-surrounding control for multiple unmanned surface vessels," *IEEE Transactions on Industrial Electronics*, vol. 69, no. 4, pp. 3988–3997, 2021.

[9] B.-B. Hu, H.-T. Zhang, W. Yao, J. Ding, and M. Cao, "Spontaneous-ordering platoon control for multirobot path navigation using guiding vector fields," *IEEE Transactions on Robotics*, 2023.

[10] C. Yang, G. N. Sue, Z. Li, L. Yang, H. Shen, Y. Chi, A. Rai, J. Zeng, and K. Sreenath, "Collaborative navigation and manipulation of a cable-towed load by multiple quadrupedal robots," *IEEE Robotics and Automation Letters*, vol. 7, no. 4, pp. 10 041–10 048, 2022.

[11] S. Xu, W. Zhang, L. Zhu, and C. P. Ho, "Distributed model predictive formation control with gait synchronization for multiple quadruped robots," in *2023 IEEE International Conference on Robotics and Automation (ICRA)*. IEEE, 2023, pp. 9995–10 002.

[12] R. T. Fawcett, L. Amanzadeh, J. Kim, A. D. Ames, and K. A. Hamed, "Distributed data-driven predictive control for multi-agent collaborative legged locomotion," in *2023 IEEE International Conference on Robotics and Automation (ICRA)*. IEEE, 2023, pp. 9924–9930.

[13] Z. Wang, Y. Torigoe, and S. Hirai, "A prestressed soft gripper: design, modeling, fabrication, and tests for food handling," *IEEE Robotics and Automation Letters*, vol. 2, no. 4, pp. 1909–1916, 2017.

[14] J. Zhu, A. Cherubini, C. Dune, D. Navarro-Alarcon, F. Alambeigi, D. Berenson, F. Ficuciello, K. Harada, J. Kober, X. Li, *et al.*, "Challenges and outlook in robotic manipulation of deformable objects," *IEEE Robotics & Automation Magazine*, vol. 29, no. 3, pp. 67–77, 2022.

[15] Z. Wang and M. Schwager, "Kinematic multi-robot manipulation with no communication using force feedback," in *2016 IEEE International Conference on Robotics and Automation (ICRA)*. IEEE, 2016, pp. 427–432.

[16] G. Loianno and V. Kumar, "Cooperative transportation using small quadrotors using monocular vision and inertial sensing," *IEEE Robotics and Automation Letters*, vol. 3, no. 2, pp. 680–687, 2017.

[17] P. Culbertson, J.-J. Slotine, and M. Schwager, "Decentralized adaptive control for collaborative manipulation of rigid bodies," *IEEE Transactions on Robotics*, vol. 37, no. 6, pp. 1906–1920, 2021.

[18] M. Manubens, D. Devaurs, L. Ros, and J. Cortés, "Motion planning for 6-d manipulation with aerial towed-cable systems," in *Robotics: science and systems (RSS)*, 2013, p. 8p.

[19] D. Sanalitro, H. J. Savino, M. Tognon, J. Cortés, and A. Franchi, "Full-pose manipulation control of a cable-suspended load with multiple uavs under uncertainties," *IEEE Robotics and Automation Letters*, vol. 5, no. 2, pp. 2185–2191, 2020.

[20] Y. Ping, M. Wang, J. Qi, C. Wu, and J. Guo, "Collaborative control based on payload-leading for the multi-quadrotor transportation systems," in *2023 IEEE International Conference on Robotics and Automation (ICRA)*. IEEE, 2023, pp. 5304–5309.

[21] H. G. De Marina and E. Smeur, "Flexible collaborative transportation by a team of rotorcraft," in *2019 International Conference on Robotics and Automation (ICRA)*. IEEE, 2019, pp. 1074–1080.

[22] S. Tang and V. Kumar, "Mixed integer quadratic program trajectory generation for a quadrotor with a cable-suspended payload," in *2015 IEEE international conference on robotics and automation (ICRA)*. IEEE, 2015, pp. 2216–2222.

[23] A. Xiao, W. Tong, L. Yang, J. Zeng, Z. Li, and K. Sreenath, "Robotic guide dog: Leading a human with leash-guided hybrid physical interaction," in *2021 IEEE International Conference on Robotics and Automation (ICRA)*. IEEE, 2021, pp. 11 470–11 476.

[24] H. Dai, A. Valenzuela, and R. Tedrake, "Whole-body motion planning with centroidal dynamics and full kinematics," in *2014 IEEE-RAS International Conference on Humanoid Robots*. IEEE, 2014, pp. 295–302.

[25] R. Grandia, F. Farshidian, R. Ranftl, and M. Hutter, "Feedback mpc for torque-controlled legged robots," in *2019 IEEE/RSJ International Conference on Intelligent Robots and Systems (IROS)*. IEEE, 2019, pp. 4730–4737.

[26] R. Grandia, F. Jenelten, S. Yang, F. Farshidian, and M. Hutter, "Perceptive locomotion through nonlinear model-predictive control," *IEEE Transactions on Robotics*, 2023.

[27] G. Lu, W. Xu, and F. Zhang, "On-manifold model predictive control for trajectory tracking on robotic systems," *IEEE Transactions on Industrial Electronics*, vol. 70, no. 9, pp. 9192–9202, 2022.

[28] D. He, W. Xu, and F. Zhang, "Symbolic representation and toolkit development of iterated error-state extended kalman filters on manifolds," *IEEE Transactions on Industrial Electronics*, 2023.

[29] H. K. Khalil and L. Praly, "High-gain observers in nonlinear feedback control," *International Journal of Robust and Nonlinear Control*, vol. 24, no. 6, pp. 993–1015, 2014.

[30] C. D. Bellicoso, C. Gehring, J. Hwangbo, P. Fankhauser, and M. Hutter, "Perception-less terrain adaptation through whole body control and hierarchical optimization," in *2016 IEEE-RAS 16th International Conference on Humanoid Robots (Humanoids)*. IEEE, 2016, pp. 558–564.

[31] Observer-based distributed mpc for collaborative quadrotor-quadruped manipulation of a cable-towed load. [Online]. Available: https://www.xushaohang.top/home/quad2_collaboration

[32] W. Xu, Y. Cai, D. He, J. Lin, and F. Zhang, "Fast-lio2: Fast direct lidar-inertial odometry," *IEEE Transactions on Robotics*, vol. 38, no. 4, pp. 2053–2073, 2022.